Conductance and conductance fluctuations of narrow disordered quantum wires

K. Nikolić and A. MacKinnon
The Blackett Laboratory, Imperial College, Prince Consort Road, London SW7 2BZ United Kingdom
(Received 31 May 1994)

In this paper we present and discuss our results for the conductance and conductance fluctuations of narrow quantum wires with two types of disorder: boundary roughness (hard-wall confining potential) and islands of strongly scattering impurities within the bulk of the wire. We use a tight-binding Hamiltonian to describe the quantum wire, infinite perfect leads, a two-terminal Landauer-type formula for the conductance, and the recursive single-particle Green's-function technique. We find that conductance quantization is easily destroyed by strong scattering. We also find that Anderson localization imposes a serious restriction on the high carrier mobility predicted in quantum wires. Conductance fluctuations in narrow quantum wires are not, in general, universal (as in the metallic regime), but can be independent of the wire length over a short range of lengths.

I. INTRODUCTION

Many unusual transport phenomena have been revealed in mesoscopic low-dimensional structures. The considerable interest in submicron electronic structures has been motivated by the expectation that potentially useful devices could be invented. Very sophisticated techniques have been developed, such as the various types of epitaxial growth, lithography, ion implantation, etching and cleaving, etc., in order to make these small size structures. However, none of them can produce perfect quantum wires. For example, GaAs/AlAs quantum well wires grown on a vicinal surface using molecular-beam epitaxy (MBE) (Ref. 1) have two characteristic types of disorder. The interface between the GaAs and the AlAs regions is not smooth and, in addition, within the region of nominally pure GaAs, there will be islands of AlAs. The question of how compositional disorder affects the transport properties of quantum wires is important.

The conductance of narrow ballistic channels, or quantum point contacts in a two-dimensional electron gas (2DEG) is quantized in integer multiples of $2e^2/h$.[2] However, this simple steplike form for the conductance as a function of the Fermi energy occurs when the transition between the wide leads and the narrow channel is adiabatic.[3] Nonadiabatic, i.e., mode-mixing transport through the constriction produces some additional features in the conductance diagram.[4,35,5] The conditions for adiabatic transport are readily achieved in the experiments. Disorder, however, can quite easily destroy conductance quantization. Poor quantization is believed to be mainly caused by backscattering. Backscattering, at low temperatures, is produced by the impurities within the wire and/or by the rough wire edge. It can also be caused indirectly through resonant states trapped in the wire, which may be created by the random field of impurities outside the wire.[7,8] However, forward scattering does not generally harm the conductance quantization, if all conducting modes are fully occupied.[8] Small-angle backscattering predominates in the highest subbands and is usually considered responsible for the destruction of the conductance quantization. When only the lowest 1D subband is occupied, however, the number of states into which an electron can be scattered by disorder is reduced. This gave rise to the prediction of a large electron mobility in a confined electron system.[9] However, the conductance is very strongly influenced by the quantum interference effects which start to emerge as elastic scattering is introduced in the ballistic regime. In the quasi-one-dimensional case there is a much higher probability of multiple scattering from the same site compared to the 2D or 3D case. This could cause Anderson localization to become dominant.

The conductance fluctuations are expected to show peculiar behavior in narrow quantum wires.[10,11] In the metallic regime all the dimensions of a sample are much larger than the mean free path l and the electron motion is well defined in all directions. Hence, the perturbation theory approach based on Feynman diagrams, which yields universal conductance fluctuations (UCF), is valid. However, the transverse quantization in quantum wires gives well resolved 1D subbands if the width of the wire (w) is smaller than the mean free path (l) and comparable to the Fermi wavelength λ_F. Therefore, in general, UCF's are not expected in quantum wires with weak disorder. On the other hand, we know that in the case of strong disorder when the wire length L becomes greater than the localization length λ, subband mixing is very strong and any quasi-one-dimensional feature of a perfect system is virtually destroyed.[12,31] Then it becomes essential to take localization effects into account. Again, application of a perturbational method[13] is inappropriate.

Here we examine the influence of rough boundaries (Sec. III), impurities (Sec. IV), and both types of disorder combined (Sec. V) on the conductance and conductance fluctuations of quantum wires at zero temperature and zero magnetic field. All calculations were done using a Landauer-type formula for the conductance.

 ©1994 The American Physical Society

II. MODEL AND METHODS

Our calculations of the conductance, described below, require detailed structural information about the quantum wire. A direct way of describing such a system would be by providing detailed geometric and structural information about an actual wire. Such data can be represented in a convenient form as a set of probability distributions and correlation functions of some basic parameters of the wire (e.g., the width, width fluctuations, confining potential, etc.). The detailed structure can be recovered, in a statistical sense, by generating wires using an appropriate algorithm and the set of probability distributions and correlation functions as an input. In order to examine the electronic properties of some realistic structures we have used structural information obtained in the Monte Carlo simulation of vicinal surface grown quantum well wires by Hugill *et al.*[14]

Quantum wires directly grown by epitaxial growth of a heterostructure, usually (Al,Ga)As, by using more or less controlled generation of terraces and steps (or corrugations) on semiconductor surfaces, seemed very attractive.[1,15–17] This process was at one time considered very promising for the eventual realization of very narrow (about a few nanometers) quantum wires.[18] More recently attention has shifted to other possibilities, such as V grooves, but as the basic principles governing the electronic structure are common to different sorts of wires we shall concentrate here on MBE grown wires. The kinetics of MBE can be successfully simulated on a computer,[14,19] provided that the values of the model parameters are correctly estimated from the experimental data. This enables one to perform Monte Carlo simulations of these wire structures and therefore, to define structural disorder in the system.[12,31] A section of a generated monolayer wire with an average width of ten lattice sites is shown in Fig. 1. The effects of the various types of compositional disorder considered here have implications for the electronic behavior of quantum wires fabricated by other techniques.

For the purpose of transport calculations the quantum wire is sandwiched between two perfect leads. The same model using a tight-binding, nearest-neighbor Hamiltonian is used to describe both the quantum wire and the leads:

$$\mathbf{H} = \sum_i |i\rangle \varepsilon_i \langle i| + \sum_{\substack{i,j \\ (i \neq j)}} |i\rangle V_{ij} \langle j|, \tag{1}$$

where $|i\rangle$ is the localized "Wannier" state or atomic orbital on site i, ε_i is the "site energy," and V_{ij} is the hopping matrix element between sites i and j. We shall assume that V_{ij} is zero unless the i and j sites are nearest neighbors, when $V_{ij} \equiv V$ (i.e., V defines our unit of energy and the effective mass).



FIG. 1. Plot of a section of the generated (real) quantum wire of average width 10, with island concentration $p = 0.05$.

We define our lead-sample-lead system to lie along the x axis. It can be divided into slices along that direction, each of which has M sites (i.e., a cross section of the quantum wire). The elastic scattering in the quantum wire (which extends from slice 1 to slice L) is described by transmission probabilities $T_{mn} = |t_{mn}|^2$, which describe the probability that an electron incident in channel (state) n on the left emerges in channel m on the right. The amplitude transmission coefficients t_{mn} can be calculated by various means. Here the formulation due to Ando[20] is used

$$t_{mn} = \sqrt{\frac{v_m}{v_n}} \{ \mathbf{U}^{-1}(+) V \mathbf{G}_{0,L+1} [\mathbf{F}^{-1}(+) - \mathbf{F}^{-1}(-)] \mathbf{U}(+) \}_{mn} , \tag{2}$$

where

$$\mathbf{F}(\pm) = \mathbf{U}(\pm) \Lambda(\pm) \mathbf{U}^{-1}(\pm), \tag{3}$$

and v_n is the longitudinal velocity in subband n. $\mathbf{G}_{0,L+1}$ is the Green's function which couples the 0th and the $(L+1)$st slice in our system (i.e., the last slice in the left lead and the first slice in the right lead). The matrices

$$\mathbf{U}(\pm) = [\mathbf{u}_1(\pm) \cdots \mathbf{u}_M(\pm)] \tag{4}$$

and

$$\Lambda(\pm) = \begin{pmatrix} \zeta_1(\pm) & & & \\ & \zeta_2(\pm) & & \\ & & \cdots & \\ & & & \zeta_M(\pm) \end{pmatrix}$$

contain the eigenvectors and eigenvalues, respectively, of the eigenvalue problem

$$\zeta \begin{pmatrix} \mathbf{C}_J \\ \mathbf{C}_{J-1} \end{pmatrix} = \begin{pmatrix} V^{-1} \left(E\mathbf{I} - \mathbf{H}_0^{(1)} \right) & -\mathbf{I} \\ \mathbf{I} & \mathbf{0} \end{pmatrix} \begin{pmatrix} \mathbf{C}_J \\ \mathbf{C}_{J-1} \end{pmatrix} . \tag{5}$$

The perfect leads extend to $-\infty$ and $+\infty$ along the x axis. In these asymptotic regions the incident and transmitted states obey the Schrödinger equation

$$(E\mathbf{I} - \mathbf{H}_J^{(1)}) \mathbf{C}_J - \mathbf{V}\mathbf{C}_{J-1} - \mathbf{V}\mathbf{C}_{J+1} = 0 , \tag{6}$$

where $\mathbf{H}_J^{(1)}$ is replaced by the Hamiltonian of an isolated ordered slice $\mathbf{H}_0^{(1)}$. $\mathbf{C}_J$ is a vector describing the amplitudes of the wave function on the Jth slice. The superscript designates the length of the system. Although $\mathbf{V}$ is generally a diagonal matrix for the nearest-neighbor, simple cubic model, in the case of purely diagonal disorder and zero magnetic field it reduces to a scalar. Due to translational invariance along the x axis, the solutions of Eq. (6) for the perfect leads, must be in the Bloch form, i.e.,

$$\zeta \mathbf{C}_{J-1} = \mathbf{C}_J , \tag{7}$$

where $\zeta = \exp(ika)$ and a is the lattice constant. The eigenvalue problem, Eq. (5), is a combination of the Schrödinger equation (6) and Eq. (7). The $2M$ eigenvalues (ζ) and eigenvectors ($\mathbf{u}$) can be separated into two groups: left-going, $\zeta(-)$ and $\mathbf{u}(-)$, and right-going waves, $\zeta(+)$ and $\mathbf{u}(+)$. If $\zeta < 1$, then from Eq. (7) the solution is exponentially decaying in the positive x direction and describes right-going evanescent modes. The $\zeta > 1$ solutions describe left-going evanescent modes. If ζ is a complex number then the classification is done according to the sign of the matrix element of the current density operator (j) (see Appendix B in Ref. 21):

$$j = \frac{e}{2i\hbar}\left[\mathbf{C}_J^\dagger \mathbf{C}_{J+1} - \mathbf{C}_J \mathbf{C}_{J+1}^\dagger + \mathbf{C}_{J-1}^\dagger \mathbf{C}_J - \mathbf{C}_{J-1}\mathbf{C}_J^\dagger\right] = \frac{2e}{\hbar}|\mathbf{C}_J|^2 \ \mathrm{Im}\,\zeta \tag{8}$$

since $|\zeta| = 1$. If $\mathrm{Im}\,\zeta > 0$ then $j > 0$ and the wave is propagating to the right, and if $\mathrm{Im}\,\zeta < 0$ then it is propagating to the left.

The Green's function $\mathbf{G}_{0,L+1}$ is calculated by using the recursive method[22]

$$\mathbf{G}_{1,N+1}^{(N+1)} = \mathbf{G}_{1,N}^{(N)} \mathbf{V}_{N,N+1} \mathbf{G}_{N+1,N+1}^{(N+1)}, \tag{9}$$

$$\mathbf{G}_{N+1,N+1}^{(N+1)} = \left[E\mathbf{I} - \mathbf{H}_{N+1}^{(1)} - \mathbf{V}_{N,N+1}^\dagger \mathbf{G}_{N,N}^{(N)} \mathbf{V}_{N,N+1}\right]^{-1}. \tag{10}$$

Iterative calculations are performed by successively adding slices to the end of the bar. This numerical technique has proved very reliable for the Anderson localization problem.[23,24] The initial conditions reflect the environment into which the wire sample is embedded. The first slice of the quantum wire (slice 1) is coupled to the end (slice 0) of the left hand lead, i.e., to a semi-infinite perfect wire. So the initial condition for calculating [$\mathbf{G}_{NN}$ in Eq. (10)] is given by the diagonal block of the Green's function ($\mathbf{G}_d^{(\infty/2)}$) at the end of a perfect bar that extends from $-\infty$ to 0 (see Ref. 22):

$$\mathbf{G}_{00} = \mathbf{G}_d^{(\infty/2)}(L\text{-lead}) = \mathbf{U}(+)\Lambda(+)\mathbf{U}^{-1}(+)V^{-1}. \tag{11}$$

Similarly for the right hand lead

$$\mathbf{G}_d^{(\infty/2)}(R\text{-lead}) = \mathbf{U}(+)\Lambda(-)\mathbf{U}^{-1}(+)V^{-1} = \mathbf{S}_\infty^{-1}, \tag{12}$$

where $\mathbf{S}_\infty^{-1}$ is the self-energy matrix, which helps us to couple the right hand lead to the other end of conductor. The effect of adding the whole right hand lead can be represented by the Hamiltonian

$$\tilde{\mathbf{H}} = \mathbf{H}_0 + \mathbf{S}_\infty$$

in the final iteration of Eq. (10). Iterations of Eq. (9) for $\mathbf{G}_{1N}$ begin with the unit matrix.

The formulation (2) can be further simplified. If $\mathbf{F}(\pm)$ is substituted by Eq. (3) and since the same eigenproblem (5) describes both left-going and right-going solutions, we get our final result:

$$t_{mn} = \sqrt{\frac{v_m}{v_n}}\ \{\ \mathbf{U}^{-1}(+)V\mathbf{G}_{0,L+1}\mathbf{U}(+)[\Lambda(-) - \Lambda(+)]\ \}_{mn}. \tag{13}$$

Note that the result is not affected by the normalization of $\mathbf{U}(\pm)$. This formulation for t_{mn} easily yields transmission probabilities for the case of a perfect wire of length L between two perfect leads of the same cross section:

$$T_{mn} = |t_{mn}|^2 = |\zeta_m(+)|^{2L}\delta_{mn}. \tag{14}$$

The conductance G, given by the two-terminal Landauer formula,[25,26] for spin-degenerate states is

$$G = 2\frac{e^2}{h}\sum_{n=1}^{N_L}\sum_{m=1}^{N_R}|t_{mn}|^2. \tag{15}$$

The summations run over the open channels, of which there are N_L in the left lead and N_R in the right lead.

The conductance fluctuations are quantified by the square root of the variance

$$\mathrm{rms}(G) = \left(\langle G^2\rangle - \langle G\rangle^2\right)^{1/2}, \tag{16}$$

where $\langle\ \rangle$ denotes averaging over an ensemble of samples, with different realizations of disorder. In our calculations all the quantum wires have a hard wall confining potential. Also for the site energy of islands $\epsilon_{\mathrm{isl}} \to \infty$ is assumed. The temperature of the system is always $T = 0$ K.

III. THE INFLUENCE OF BOUNDARY ROUGHNESS

For the investigation of the transport properties of quantum wires with rough edges we use the geometry of the system which is shown at the top of Fig. 2. The average value of the width is taken to be $\langle w\rangle = 10$ and the width of the leads will be fixed at $W = 20$ throughout this section. Here we shall analyze results for four types of calculation: conductance of a single quantum wire and ensemble average quantities related to the conductance, as functions of Fermi energy E and wire length L. First, we discuss the results for the conductance of a single quantum wire sample, presented in Fig. 2.

The edge roughness destroys the conductance quantization steps, first near the band center for very small disorder (see case $L = 5$ in Fig. 2). The deterioration of the quantization spreads towards the band edge both as the disorder and as the length of the wire is increased. In the mesoscopic regime, when $l < L < \lambda$, the conductance curve shows sample specific fluctuations as a function of energy and length. However, the amplitude of these fluctuations is of order e^2/h, independent of energy (Fig. 2, $L = 10, 30$) or length (see inset of Fig. 2). This is a quantum interference effect similar to the universal conductance fluctuations observed in the mesoscopic regime[27] of other systems. The particular value for the conductance is determined by the electron wavelength (i.e., electron energy), the length of the quantum wire and the actual realization of the disorder in a sam-

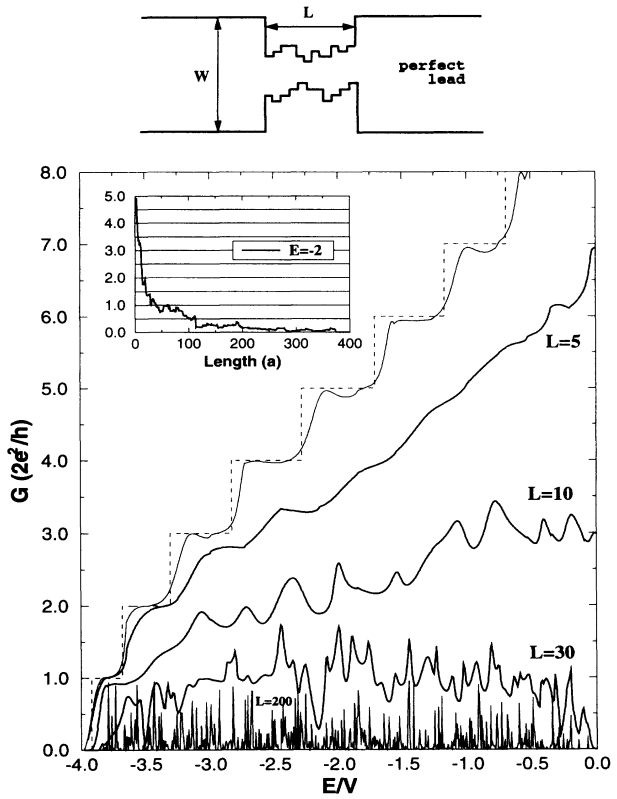


FIG. 2. G as a function of energy of a single sample of quantum wire with rough edges and no island disorder, for wire lengths: $L = 5$, 10, 30, and 200, and average wire width $\langle w \rangle = 10$ and leads width $W = 20$. Reference step functions are the conductances of the perfect wire of the width $w = 10$, length $L = 5$, and leads with $W = 20$ (full line), and $W = 10$ (i.e., no difference between leads and wire—broken line). The inset is the conductance of a quantum wire sample as a function of the wire length. The top picture shows the geometry of the lead-wire-lead system used in the calculations.

ple. The conditions for the destructive or constructive interference of an electron wave front are, generally, very sensitive to all of these parameters. The scale of the sensitivity to energy, however, differs with the length of the wire (which is evident from Fig. 2 for $L = 10$ and 30) or with the level of disorder. This observation supports the idea that the fluctuations do not arise from classical scattering from the rough boundary but from the phase modulation of the electron wave function due to multiple elastic scattering in the wire.[28] We estimate that the typical spacing between peaks and valleys in the conductance as a function of energy depends on the wire length as $E_c \sim 1/L$. This is a weaker dependence on the wire length than in the case of the universal conductance fluctuations in the metallic regime, where $E_c \sim 1/L^2$ (Ref. 27). It should also be noted that the conductance falls faster near the band center than elsewhere (this will be clear from the results for the average conductance). When the system is in the strong localization regime, the conductance is reduced to a set of peaks of different amplitudes, with maximum value of $2e^2/h$ (see Fig. 2, $L = 200$). The mechanism of electron transport is resonant tunneling through the quantum wire.[29] When the energy of an electron coincides with an eigenenergy of the wire the electron can be transmitted through the wire via this localized state. The height of the peak of G depends on the overlap between the wave functions of this spatially localized state inside the wire and the propagating states in the leads. As the length of the wire is further increased, the number of peaks and their amplitudes reduce and their positions change. The highest such peaks are probably due to tunnelling through multiple resonant states, so-called "necklace" states.[36]

Next we discuss the results for the ensemble average conductance and for the conductance fluctuations. Figure 3 shows results for $\langle G \rangle$ and $\exp(\langle \ln G \rangle)$. Conductance quantization disappears very quickly, although the presence of a short plateau for the first subband can be observed for the shorter wires. The boundary roughness has less impact for longer wavelengths (smaller energies) and hence the average conductance tends to decrease with increasing energy. As the length of the wire increases there is a rapid decrease of G near the band center. In the strong localization regime, a broad peak emerges near the band edge (see Fig. 3 for $L = 100$), which corresponds to the peak in the localization length.[31] In this regime, the average conductance of quasi-one-dimensional systems falls off exponentially with the length:[30]

$$G(E, L) \sim \exp\left(-2L/\lambda(E)\right) . \tag{17}$$

The conductance fluctuations for the case of the quantum wire with boundary roughness only, calculated for the examples from Fig. 3 by using definition Eq. (16), are presented in Fig. 4. Three characteristic regimes are shown.

(1) The quasiballistic regime—the wire length is comparable with the mean free path length, $L \simeq l$ (e.g.,

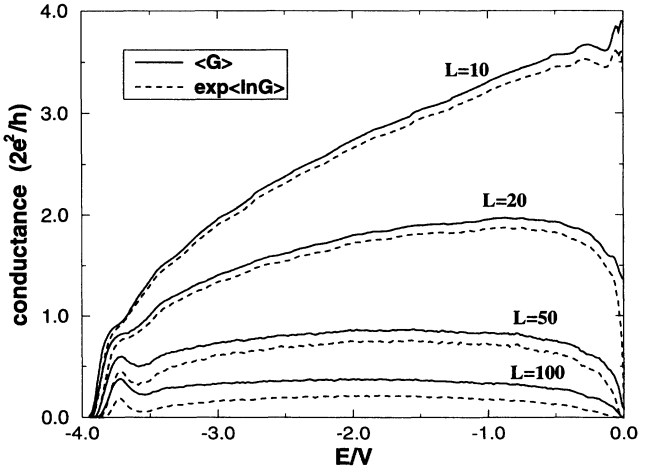


FIG. 3. Average conductance as a function of energy, for quantum wires with rough boundary and no island disorder, for different wire lengths: $L = 10$, 20, 50, and 100. Number of samples taken for calculating average values are $N = 1000, 1000, 3000, 4000$ for wire lengths $L = 10, 20, 50, 100$, respectively.

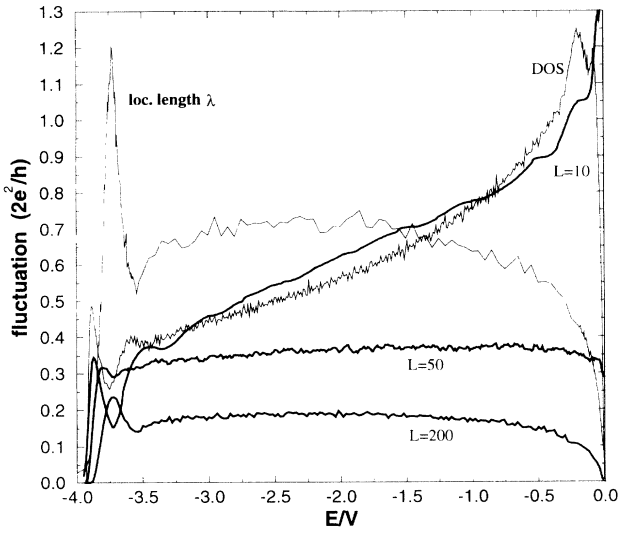


FIG. 4. Conductance fluctuations which correspond to the case in Fig. 4 for the wire lengths: $L = 10$, 50, and 200 (three bold lines). Two thin lines are the localization length and the density of states (both rescaled: $\lambda \rightarrow \lambda/100$ and DOS $\rightarrow$ DOS$*5$) for quantum wires with boundary roughness.

$L = 10$ for most of the energies and for the level of disorder assumed in our samples);

(2) the mesoscopic regime where the wire length is $l < L < \lambda$ (e.g., $L = 50$);

(3) the strong localization regime—$L > \lambda$ (e.g., $L = 200$).

Since the elastic mean free path and the localization length are both functions of energy, a particular wire can move between these regimes as the energy is changed. The fluctuations for the case $L = 10$ in Fig. 4 show interesting similarities with the density of states for the same type of quantum wires. There is a peak near the band edge which corresponds to the peak in the density of states (DOS), which is the last remaining feature of the inverse square root singularities from the DOS of clean quasi-one-dimensional systems (see Ref. 31). This behavior can be explained in the following way. For short wires (i.e., quasiballistic transport) the important length is the elastic mean free path l. If l increases (as a function of energy) in the quasiballistic regime, then the conductance fluctuations decrease—as the scattering in the wire is reduced, and vice versa. Since l is roughly inversely proportional to the DOS (when the DOS is increased the scattering rate increases and therefore l decreases), then the conductance fluctuations might be expected to mirror the DOS. As L is increased with respect to l (and still $L << \lambda$) then the fluctuations will increase towards their maximal value, which is reached in the mesoscopic regime. The quantum wires of length $L = 50$ in Fig. 4 show a relatively wide region of energy in which the conductance fluctuations are independent of energy, with a value which is close to the universal value for quasi-one-dimensional systems [$\mathrm{rms}(G) = 0.729e^2/h$ (Ref. 27)].

For long wires ($L = 200$) we have the strong localization regime and $\mathrm{rms}(G(E))$ follows the curve for the localization length $\lambda(E)$ (see Fig. 4), i.e., the average conductance, since these are related [Eq. (17)]. That $\mathrm{rms}(G)$ and $\langle G \rangle$ are proportional can be understood by using the picture of "open" and "shut" channels, or "maximal fluctuations," in a quantum wire in the strong localization regime.[32] This terminology is associated with the distribution function $P(\tau)$ for the eigenvalues τ ($0 \leq \tau \leq 1$) of $\mathbf{t}\mathbf{t}^\dagger$, where $\mathbf{t}$ is the transmission matrix: it has a peak at $\tau = 0$, and a tail which extends to $\tau = 1$.[32,33] Each eigenvector of $\mathbf{t}_L\mathbf{t}_L^\dagger$ defines a conducting "microchannel" with the corresponding conductance τ in units of $(2)e^2/h$.[32] As the size of the system is increased, the peak at $\tau = 0$ strengthens at the expense of the tail, but the shape of the tail remains the same.

For long lengths, therefore, most of the microchannels will have conductance of order 0 since the bulk of the distribution is around 0. Only a small fraction of the channels, with values for τ of order 1 (roughly $0.1 < \tau \leq 1$), will contribute to the conductance. Such a distribution of τ implies that the fluctuations tend to the maximum possible value consistent with their mean. However, the moments of the conductance, $\langle (\mathrm{Tr}\,\mathbf{t}\mathbf{t}^\dagger)^n \rangle$, for 2D and 3D cases do not show the same size dependence as the moments of $\mathrm{Tr}\langle (\mathbf{t}\mathbf{t}^\dagger)^n \rangle$, within the metallic regime. Universal conductance fluctuations are affected by the correlations between the τs rather than by the distribution of the τs themselves. Universal conductance fluctuations are restricted to disordered systems in the metallic regime where perturbation theory is applicable. When localization effects are important, however, the correlations between the microchannels change and a different sort of fluctuations is observed.[32] The statistics of a single microchannel were found to be crucial in the strong localization regime.

The average conductance of the disordered quasi-one-dimensional system shows an asymptotically exponential decrease with the length.[30] This single parameter dependence suggests that the conductance statistics of quasi-one-dimensional samples, with a length much longer than the localization length, is dominated by a single channel. Hence a similar size dependence for the conductance moments should be expected as for $\mathrm{Tr}\langle (\mathbf{t}\mathbf{t}^\dagger)^n \rangle$, since the distribution of τs is important, rather than the correlation between them. This picture of the conductance statistics in the strong localization regime shows that the conductance fluctuations are proportional to the average conductance.

In Fig. 5 results are given for the conductance as a function of wire length, for a fixed energy. The results for the average conductance are presented for two values of the energy and two more examples of conductance fluctuations are added. The decrease of conductance is more marked in the quasiballistic (near ballistic) regime (short wires), where the difference between $\langle G \rangle$ and $\exp(\langle \ln G \rangle)$ is negligible. The difference between the two averages increases as the disorder or length of the wire is increased (Figs. 3 and 5). This shows that the average $\langle G \rangle$ is dominated by a small number of samples with conductance of order $2e^2/h$. The divergence of the two curves indicates that the conductance distribution is transforming to the form which has a peak for small conductances and a long

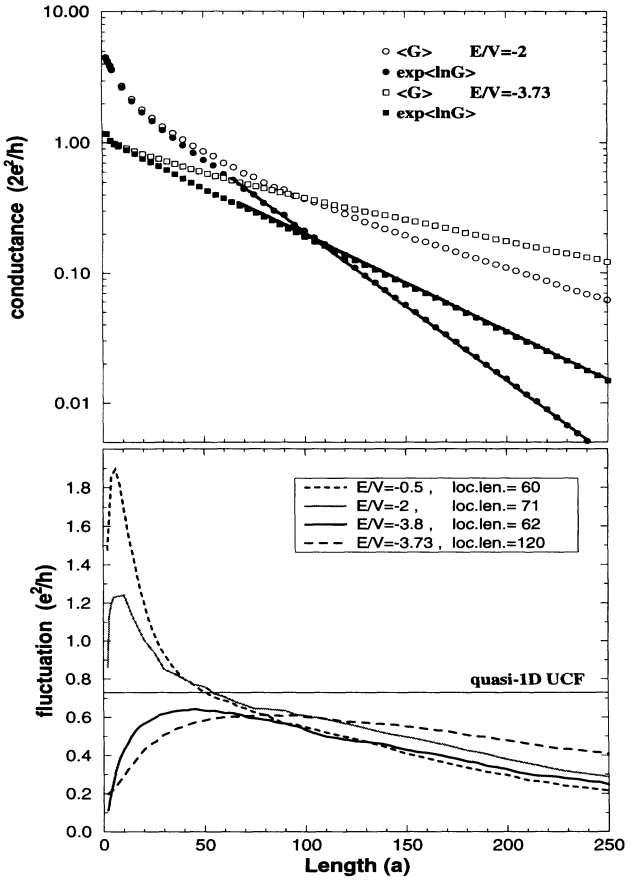


FIG. 5. Average conductance as a function of wire length for real wire without islands for energies $E = -2$ and -3.73—top figure. The corresponding conductance fluctuations are shown in the lower figure as well as fluctuations for energies $E = -0.5$ and -3.8. Number of samples is $N = 4000$.

tail towards larger conductances, i.e., it is transforming to a log-normal distribution.[30] For wires of length $L > \lambda$ the decrease of the average conductance $\exp(\langle \ln G \rangle)$ with the length of the wire is mainly determined by the localization length. The value for the localization length can be obtained from Fig. 5, where $\langle \ln G \rangle$ is fitted with a straight line and λ is determined from its slope,

$$\lambda = -\frac{\partial \langle \ln G \rangle}{2 \partial L} \tag{18}$$

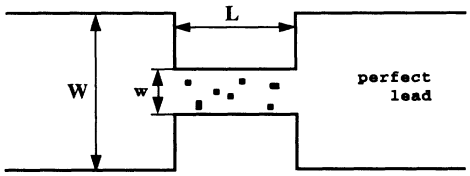
for wires of length $L >> \lambda$.

The results for the conductance fluctuations are also shown in Fig. 5. The fluctuations first increase for very short wire lengths ($L < 10$). This is the nearly ballistic regime where the fluctuations grow as the disorder (or wire length) increases. On the other side, for long wires, i.e., the strong localization regime ($L > \lambda$), the fluctuations decrease as the wire becomes longer, due to the overall decrease of the conductance. In this regime the fluctuations between wires of the same length depend only on the localization length (see Fig. 5). The fluctuations take maximal values between these two regimes. Fluctuations for wires with many subbands ($E = -0.5$ and -2 in Fig. 5) have a sharp peak for short lengths and then start to decrease well before the wire has become longer than λ. The fluctuations in the wires with a few subbands ($E = -3.73$ and -3.8 in Fig. 5) even appear to be independent of length for several ranges of L in the intermediate region. This could be called the universal region,[11,10] although the constant value of the conductance fluctuations is not equal to the universal value obtained for quasi-one-dimensional systems in the perturbation theory.[27]

IV. THE INFLUENCE OF ISLANDS

The effects of the strong scattering centers (i.e., islands) in the bulk of the quantum wire are examined for the case of an otherwise perfect wire with islands for the system geometry shown in Fig. 6. As in the case of rough boundaries, we consider the conductance of individual samples as well as the average conductance as a function of energy or wire length.

The conductance of a single sample of a quantum wire with islands is shown in Fig. 6. Even a small concentration of islands causes an almost complete suppression of the conductance quantization. In Fig. 6 one can compare the results for a quantum wire of length $L = 4$ with island concentration $p = 5\%$ (which means only two islands at random positions) with the conductance for a



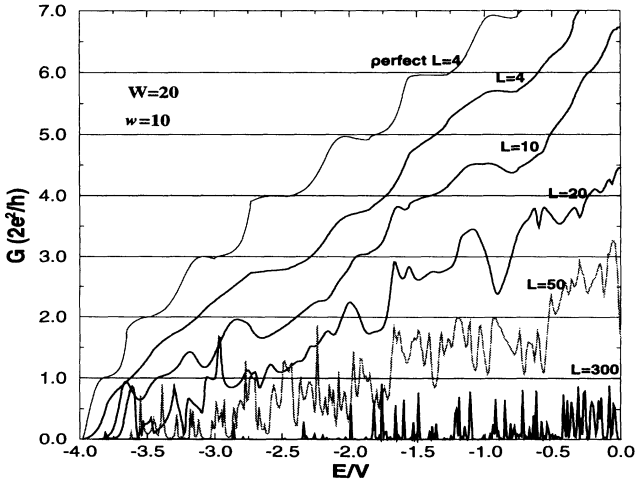


FIG. 6. G as a function of energy for a single sample of perfect quantum wire (width $w = 10$) with island disorder, for different wire lengths: $L = 4$, 10, 20, 50, and 300. Island concentration is $p = 5\%$. Also is presented conductance for perfect constriction of length $L = 4$ and width $w = 10$. The top figure shows the geometry of the system.

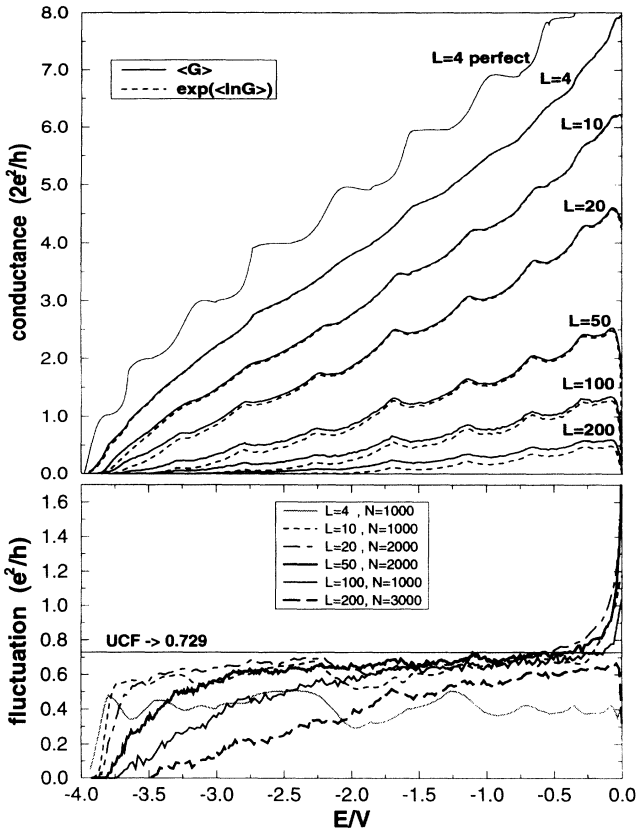


FIG. 7. Energy dependence of the average conductance and conductance fluctuations of a perfect wire with islands. Wire lengths are $L = 4, 10, 20, 50, 100, 200$. Island concentration is $p = 5\%$, $W = 20$ and wire width is $w = 10$. Number of samples taken for calculating average values is N. The universal value for UCF of quasi-one-dimensional metallic wires is marked by a horizontal line.

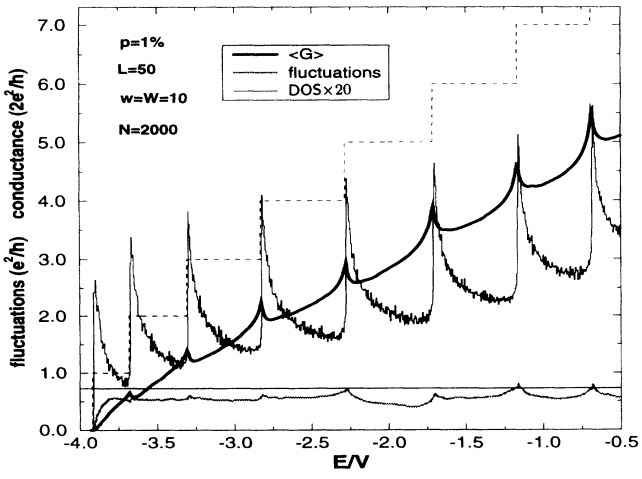


FIG. 8. $\langle G(E)\rangle$ and rms$(G(E))$ for a perfect wire with island concentration $p = 1\%$. Steps represent the conductance for the case of perfect wire. (Note the different units for $\langle G\rangle$ and fluctuations.) The histogram of the (rescaled) DOS for this wire is also shown.

perfect wire of length $L = 4$. Island disorder reduces the conductance in a similar way in each subband. In the mesoscopic regime, where $l < L < \lambda$ (examples $L = 20$ and 50 in Fig. 6), the conductance fluctuates as a function of energy. These fluctuations are of the order e^2/h. This is a quantum interference effect in which the scale of the sensitivity to changes in the energy depends on the length of the wire. We estimate that this dependence is of the form $E_c \sim 1/L^2$, i.e., similar to UCF, and differs from that of the fluctuations in the quantum wire with rough boundaries (Sec. III). E_c is the change of the Fermi energy needed to modify the relevant phase differences across the sample by about 2π. The fluctuation of the conductance between different samples is also of order e^2/h. In the strong localization regime (e.g., case $L = 300$ in Fig. 6) the conductance is reduced to a set of peaks of maximum amplitude $2e^2/h$. Each peak corresponds to the occurrence of resonant tunnelling through the wire. The localization length generally increases as energy grows and therefore the peaks get higher towards the center of the band.

The average conductance for the case of bulk (island)

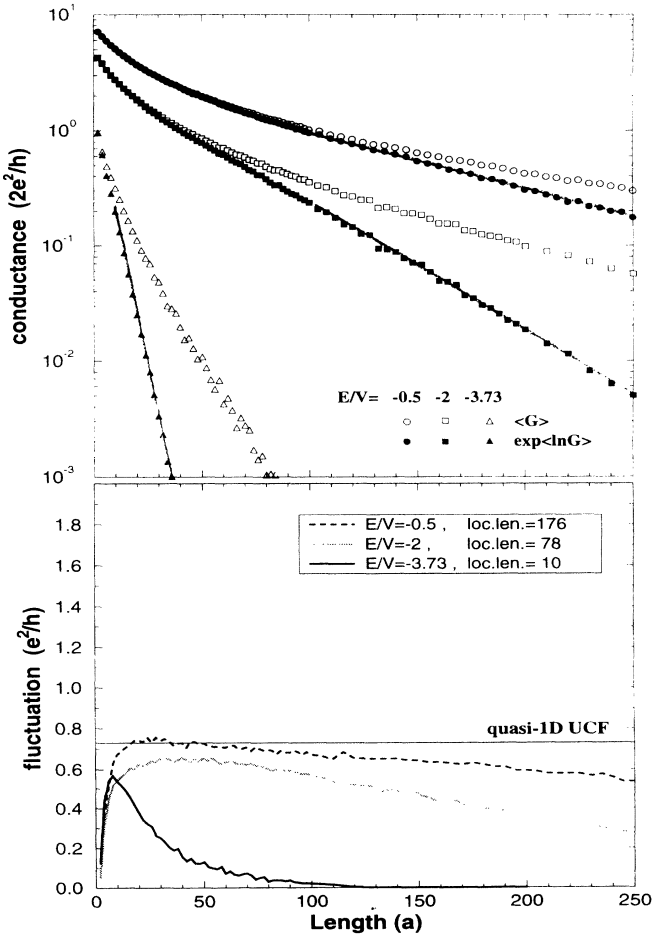


FIG. 9. Average conductance as a function of wire length for perfect wire with islands (concentration $p = 5\%$) for energies $E = -0.5$, -2, and -3.73—upper figure. The corresponding conductance fluctuations are shown in the lower figure. The number of samples is $N = 4000$, $W = 20$, and $w = 10$.

disorder is shown in Figs. 7 and 9. This type of disorder has a similar effect on each subband, unlike the case of edge roughness where higher subbands are more affected than lower ones. The average conductance as a function of energy exhibits local maxima near the energies of the subband edges of the perfect wire (Figs. 7 and 8). This becomes more obvious for the smaller concentrations of islands (e.g., the island concentrations are $p = 5\%$ in the case presented in Fig. 7 and $p = 1\%$ in Fig. 8).

The behavior of the average conductance of a disordered quantum wire modeled by the (Anderson) Hamiltonian with a uniform distribution for the site energies of the wire[34] is, to some extent, similar. Although the general appearance of the curves differs (for the strong-scattering regime it looks like a line with peaks, whereas for the Anderson model it looks like a line with dips), in both cases the DOS is connected to $\langle G(E)\rangle$ in the same way. Electron scattering is proportional to the number of available states into which an electron can be scattered, i.e., to the DOS. Therefore the electron mobility and conductance should decrease when the DOS increases and vice versa, see Fig. 8.

The average conductance decreases exponentially with the length of the wire, see Fig. 9, which is the expected behavior for the localized states. The slope of the line $\exp(\langle \ln(G)\rangle)$ for long wires determines the localization length for any energy, as defined by the Eq. (18).

The conductance fluctuations first increase in the quasiballistic regime (Fig. 9), go through a maximum in the region $l < L < \lambda$ and then decrease as the length of the wire increases. The decrease is slower for energies with longer localization lengths. A short region of lengths, where fluctuations are almost independent of the wire length, can be observed for the energies $E = -0.5$ and -2. The level of the fluctuations in this universal region depends on energy and it is not, in general, equal to UCF value for quasi-one-dimensional metallic systems. However, by chance we have found a case (that is $E = -0.5$ in Fig. 9) where $\mathrm{rms}(G) \approx 0.73$. The conductance fluctuations (Fig. 7) increase with the energy and tend to a sort of asymptotical value. This value is close to the UCF constant for wires with lengths inside the region $l < L < \lambda$, and decreases as the wire lengths move out of this region.

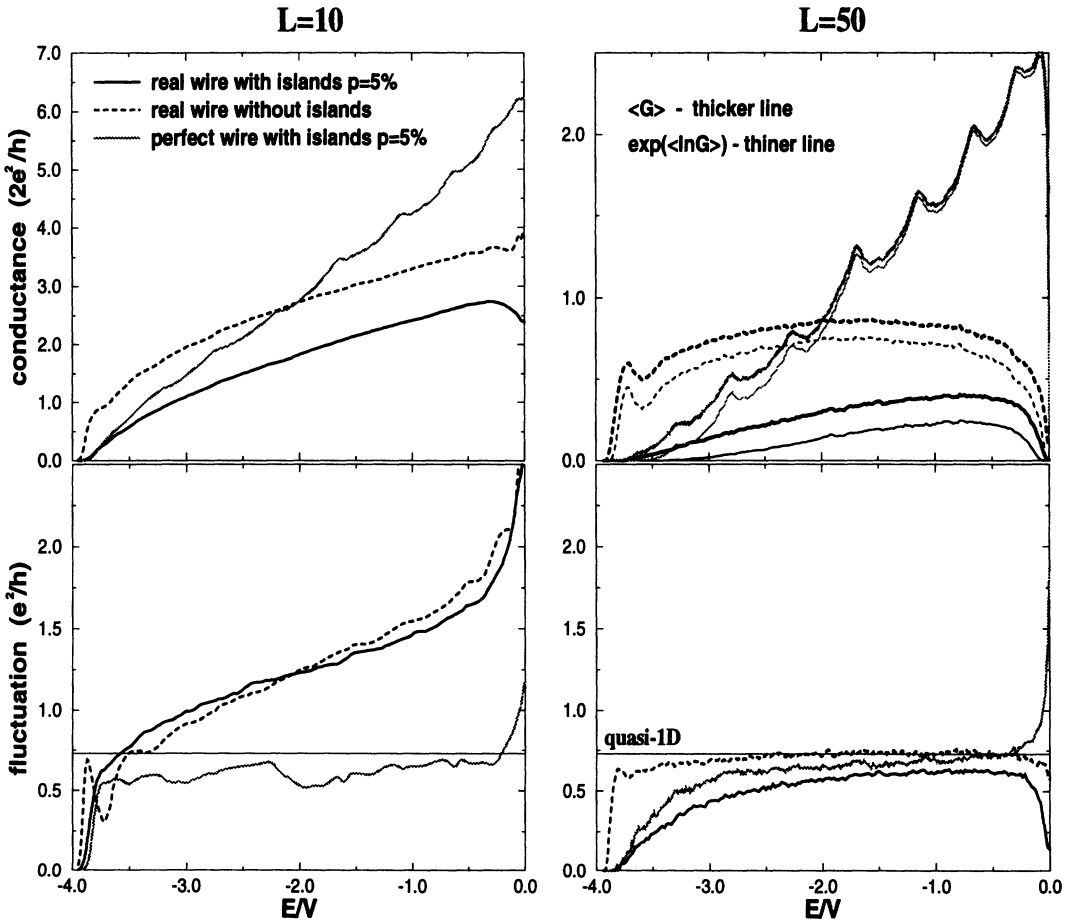


FIG. 10. The average conductance and the conductance fluctuations as function of energy for real wire with islands, $p = 5\%$ (black full line), for wire lengths $L = 10$ and 50. These results can be compared with the results for the case of real wire without islands (i.e., wire with rough edges), $W = 20$, $\langle w\rangle = 10$, and perfect wire with islands of concentration $p = 5\%$ and $W = 20$, $w = 10$. For wire length $L = 10$, $\langle G\rangle$ and $\exp(\langle \ln G\rangle)$ are virtually the same, so only $\langle G\rangle$ is shown, whereas for $L = 50$ both averages are shown. Number of samples are $N = 1000$ ($L = 10$) and $N = 3000$ ($L = 50$).

V. REAL WIRES WITH ISLANDS

So far we have examined separately the effects of boundary roughness and islands on the quantum wire conductance. Real wires with islands have both types of disorder. The geometry of the system used for the calculation of the conductance is the same as in the case of real wires without islands, shown at the top of Fig. 2.

Some results for the average conductance and fluctuations as functions of energy are shown in Fig. 10 for two lengths of wire, $L = 10$ and 50. The average conductance for both regimes shows no features, just a monotonically rising curve which bends and falls off near the band center. The presence of both types of disorder causes a further decrease of the conductance when compared with a wire with only one type of disorder. One can say that the influence of islands is dominant for energies near the band edge, whereas the influence of edge roughness becomes dominant towards the band center. Any feature of the conductance quantization for a single sample is quickly destroyed by the presence of both types of disorder. The conductance fluctuations for nearly ballistic samples ($L = 10$) have similar values to the fluctuations for the case of a real wire without islands, except for energies near the band edge. However, as the wire length increases the conductance fluctuations for a real wire with islands decreases faster then for the case without islands. This is because strong localization sets in sooner in the presence of islands. It was found in Ref. 31 that the localization length of real wires with islands is usually about half of the localization length of real wires without islands (case of $p = 5\%$ island concentration).

The conductance fluctuations as a function of length behave like the conductance fluctuations for the case of a perfect wire with islands for energies near the band edge, but for higher energies they are similar to the case of real wires without islands.

VI. DISCUSSION AND CONCLUSION

The characteristic coherent transport regimes (quasiballistic, mesoscopic—$l < L < \lambda$ and strong localization) are each affected by disorder in a similar way. For boundary roughness the influence is weak near the band edge, and increases as the energy increases. However, the influence of the island disorder is strongest on the highest propagating modes and does not depend on the mode (subband) number. Since the total conductance increases with the number of propagating modes, then, in general, the average conductance increases with the energy. But note that the average conductance, as a function of energy, always drops when a new subband opens due to the enhanced intersubband scattering. This was not observed for the case of boundary roughness only. For the quasiballistic regime the conductance quantization deteriorates very rapidly as the number of scattering events increases. The average conductance decays exponentially as a function of wire length (for $L > \lambda$), for any kind of disorder, which is considered as an additional confirmation of the exponential localization of electron states. Anderson localization is very effective in reducing the carrier mobility in narrow quantum wires. This effect acts strongly against the predicted high mobility for quantum wires.[9]

The conductance fluctuations of narrow quantum wires depend, in general, on the length of the wire, and are therefore not universal conductance fluctuations (UCF). However, the case with rough edges can show a universal region, but only for energies in the first subband. The value for rms(G) is not far from the UCF value for metallic quasi-one-dimensional systems ($0.729e^2/h$) and depends on the energy. An increase in the localization length extends this region of constant fluctuations. Ando and Tamura[11] have predicted that for wider wires than we have, a much broader region of universal conductance fluctuations will appear. We find, on the contrary, that for island disorder short universal regions can exist only for higher energies and the actual value for rms(G) approaches the UCF as the energy increases. The universal region, if it exists, appears for wires of length $l < L < \lambda$, and the fluctuations reach a maximum in this region.

Changing the cross section of the leads makes no qualitative difference to the conductance of a system consisting of a disordered wire attached to two perfect leads.[5] Some small quantitative changes are observed only when $W \sim w$ (which will be reported elsewhere). In any case, the conductance becomes independent of W when $W >> w$. This should be expected, since for large values of W, transverse modes in the leads are densely distributed, and there are many of them contributing to the total conductance.[35]

[1] P. M. Petroff, A. C. Gossard, and W. Weigmann, Appl. Phys. Lett. **45**, 620 (1984).
[2] B. J. van Wees, H. van Houten, C. W. Beenakker, J. G. Williamson, L. P. Kouwenhoven, D. van der Marel, and C. T. Foxton, Phys. Rev. Lett. **60**, 848 (1988); D. A. Wharam, T. J. Thornton, R. Newbury, M. Pepper, H. Ahmed, J. E. F. Frost, D. G. Hasko, D. C. Peacock, D. A. Ritchie, and G. A. C. Jones, J. Phys. Condens. Matter **21**, L209 (1988).
[3] L. I. Glazman, G. B. Lesovik, D. E. Khmel'nitskii, and R. I. Shekhter, Pis'ma Zh. Eksp. Teor. Fiz. **48**, 218 (1988) [JETP Lett. **48**, 239 (1988)]; L. I. Glazman and M. Jonson, Phys. Rev. B **41**, 10 686 (1990).
[4] G. Kirczenow, Solid State Commun. **68**, 715 (1988); Phys. Rev. B **39**, 10 452 (1989); A. Szafer and A. D. Stone, Phys. Rev. Lett. **62**, 300 (1989); Song He and S. Das Sarma, Phys. Rev. B **48**, 4629 (1993).
[5] K. Nikolić, Ph.D. thesis, Imperial College, London, 1993.
[6] G. Timp, in *Physics of Nanostructures*, edited J. H. Davies

and A. R. Long, Proceedings of the 38th Scottish Universities Summer School in Physics (Institute of Physics, Bristol, 1992).
[7] J. A. Nixon, J. H. Davies, and H. U. Baranger, Phys. Rev. B **43**, 12 638 (1991).
[8] M. J. Laughton, J. R. Barker, J. A. Nixon, and J. H. Davies, Phys. Rev. B **44**, 1150 (1991).
[9] H. Sakaki, Jpn. J. Appl. Phys. **19**, 94 (1980).
[10] H. Tamura and T. Ando, Phys. Rev. B **44**, 1792 (1991).
[11] T. Ando and H. Tamura, Phys. Rev. B **46**, 2332 (1992).
[12] J. P. G. Taylor, K. J. Hugill, D. D. Vvedensky, and A. MacKinnon, Phys. Rev. Lett. **67**, 2359 (1991).
[13] A. D. Stone, in *Physics of Nanostructures*, edited by J. H. Davies and A. R. Long, Proceedings of the 38th Scottish Universities Summer School in Physics (Institute of Physics, Bristol, 1992).
[14] K. J. Hugill, S. Clarke, D. D. Vvedensky, and B. A. Joyce, J. Appl. Phys. **66**, 3415 (1989).
[15] T. Fukui and H. Saito, Appl. Phys. Lett. **50**, 824 (1987).
[16] M. S. Miller, H. Weman, C. E. Pryor, M. Krichnamurthy, P. M. Petroff, H. Kroemer, and J. L. Merz, Phys. Rev. Lett. **68**, 3464 (1992).
[17] R. Nötzel, N. N. Ledentsov, L. Däweritz, M. Hohenstein, and K. Ploog, Phys. Rev. Lett. **67**, 3812 (1991).
[18] These widths of about 10 nm yield a subband separation of $\sim$ 100 meV for the lateral confinement potential of several hundred meV.
[19] B. A. Joyce, J. H. Neave, J. Zhang, D. D. Vvedensky, S. Clarke, K. J. Hugill, T. Shitara, and A. K. Myers-Beaghton, Semicond. Sci. Technol. **5**, 1147 (1990).
[20] T. Ando, Phys. Rev. B **44**, 8017 (1991).
[21] H. U. Baranger and A. D. Stone, Phys. Rev. B **40**, 8169 (1989).
[22] A. MacKinnon, Z. Phys. B **59**, 385 (1985).
[23] A. MacKinnon and B. Kramer, Phys. Rev. Lett. **47**, 1546 (1981).
[24] C. M. Soukoulis, I. Webman, G. S. Grest, and E. N. Economou, Phys. Rev. B **26**, 1838 (1982); A. D. Zdetsis, C. M. Soukoulis, E. N. Economou, and G. S. Grest, *ibid.* **32**, 7811 (1985).
[25] R. Landauer, IBM J. Res. Dev. **1**, 223 (1957); Philos. Mag. **21**, 863 (1970).
[26] D. S. Fisher and P. A. Lee, Phys. Rev. B **23**, 6851 (1981).
[27] P. A. Lee and A. Douglas Stone, Phys. Rev. Lett. **55**, 1622 (1985); P. A. Lee, A. D. Stone, and H. Fukuyama, Phys. Rev. B **35**, 1039 (1987).
[28] Y. Takagaki and D. K. Ferry, J. Phys. Condens. Matter **4**, 10 421 (1992); Phys. Rev. B **46**, 15 218 (1992).
[29] G. W. Bryant, Phys. Rev. B **44**, 12837 (1991).
[30] R. Johnston and H. Kunz, J. Phys. C **16**, 3895 (1983).
[31] K. Nikolić and A. MacKinnon, Phys. Rev. B **47**, 6555 (1993).
[32] J. B. Pendry, A. MacKinnon, and P. J. Roberts, Proc. R. Soc. London Ser. A **437** (1992).
[33] A. MacKinnon, in *Quantum Coherence in Mesoscopic Systems*, edited by B. Kramer (Plenum Press, New York, 1991), pp. 415–427.
[34] J. Mašek and B. Kramer, J. Phys. Condens. Matter **1**, 6395 (1989).
[35] A. Szafer and A. D. Stone, Phys. Rev. Lett. **62**, 300 (1989).
[36] J. B. Pendry, J. Phys. C **20**, 733 (1987).

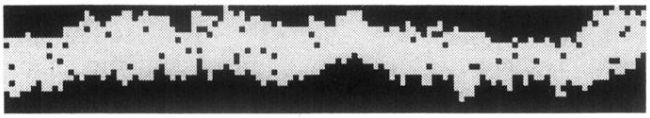


FIG. 1. Plot of a section of the generated (real) quantum wire of average width 10, with island concentration $p = 0.05$.